We are IntechOpen, the world's leading publisher of Open Access books Built by scientists, for scientists

6,900
Open access books available

185,000
International authors and editors

200M
Downloads

Our authors are among the

154
Countries delivered to

TOP 1%
most cited scientists

12.2%
Contributors from top 500 universities



WEB OF SCIENCE™

Selection of our books indexed in the Book Citation Index in Web of Science™ Core Collection (BKCI)

Interested in publishing with us?
Contact book.department@intechopen.com

Numbers displayed above are based on latest data collected.
For more information visit www.intechopen.com



14

Evolution of Optical Sampling

Gianluca Berrettini[1], Antonella Bogoni[2], Francesco Fresi[1],
Gianluca Meloni[2] and Luca Potì[2]
[1]*Scuola Superiore Sant'Anna, Pisa,*
[2]*CNIT - Photonic Networks National Laboratory,*
Via G. Moruzzi 1, 56124 Pisa,
Italy

1. Introduction

The need of direct measure and monitoring of ultra-fast signal in the time domain is rapidly increasing, being of interest in a large number of applications such as ultra-fast communication, biophotonics, sensing, large systems synchronization, dynamic characterization and testing of new materials. In particular in the telecommunication field optical sampling can been exploited for high bit rate waveform and eye diagram measurements, time resolved state of polarization monitoring, and investigation of fiber transmission impairments.
Microwave digital sampling techniques are evolved into powerful tools for resolving signals up to 100 GHz (Agoston et al., 2003), but electronic bandwidth limitations still remain.
Nowadays digital sampling operations in the optical domain look like an effective alternative solution for increasing the sampling bandwidth and resolve signals up to 640 Gb/s and beyond. In the optical sampling techniques system, the optical signal is sampled in the optical domain by an optical sampling gate. Only then, the resulting samples are converted to an electrical signal and detected. In this case the need for high bandwidth electronics is circumvented and the bandwidth of the measurement instrument is only limited by the optical sampling gate.
Up to now different kinds of optical sampling techniques have been proposed in order to study the behavior of ultra-fast optical signals. Many solutions implement a synchronous sampling that may enable low jitter, high resolution and high accuracy. This technique needs a clock recovery system to synchronize the optical sampling pulses to the signal under test; however, when the data rate or repetition rate of the analyzed signal is very high, the development of the synchronization circuitry can be very critical and expensive. In particular, in case of repetition rates beyond 100 GHz, some all-optical clock recovery solutions have to be adopted (Yamamoto et al., 2001; Tong et al., 2000; Uhua et al., 2003), but which are still far from being technologically consolidated. Other optical sampling schemes carry out an asynchronous sampling exploiting sophisticated electronics for the generation of a sampling gate (Shake et al., 2003a). Optical asynchronous sampling has been successfully demonstrated for signal up to 160 Gbit/s in (Westlund et al., 2005 a,b), where the capability of the optical sampler to estimate the Q value and the performances of the

Source: Advances in Lasers and Electro Optics, Book edited by: Nelson Costa and Adolfo Cartaxo,
ISBN 978-953-307-088-9, pp. 838, April 2010, INTECH, Croatia, downloaded from SCIYO.COM

exploited nonlinearity are investigated, confirming the high potentialities of an asynchronous sampling technique.
Finally, quasi-synchronous optical sampling has been demonstrated for 640 Gb/s optical time division multiplexing (OTDM) signals without data-post processing (Fresi et al., 2008). Independently on the sampling technique, the optical sampling operation requires a nonlinear interaction between the signal to be resolved and an ultra-short pulse train that act as sampling signal. Such nonlinear process can be generated in different nonlinear elements as highly non linear fiber (HNLF) (Malacarne et al., 2007; Watanabe et al., 2004; Schmidt et al., 2002a), nonlinear crystals and waveguides (Nogiwa et al., 2000; Takara et al., 1996a; Kawanishi et al., 2001) or semiconductor devices (Maguire et al., 2005; Shirane et al., 2000). Fibers, crystals and waveguides may enable ultra-fast dynamics and high efficiency, while semiconductor devices could reduce the power consumption.

2. Digital sampling operation

In contrast to an analog oscilloscope, a sampling oscilloscope acquires the waveform as a series of samples, and stores these samples until it accumulates enough samples to describe a waveform. Conventional electronic digital sampling oscilloscopes use analod to digital convertersi (ADC) to sample the signal at discrete points in time and convert the signal's voltage at these points into digital values called sample points. The sample clock determines how often the ADC takes a sample. This rate is referred to as the sample rate and is expressed in samples per second (S/s). Although there are a number of different implementations of sampling technology, today's digital oscilloscopes utilize two basic sampling methods: real-time sampling and equivalent-time sampling. Equivalent-time sampling can be divided further, into two subcategories: random and sequential. Each method has distinct advantages, depending on the kind of measurements being made.
Real-time sampling is ideal for signals whose frequency range is less than half the oscilloscope's maximum sample rate. Here, the oscilloscope can acquire more than enough points in one "sweep" of the waveform to construct an accurate picture. Real-time sampling is the only way to capture fast, single-shot, transient signals with a digital oscilloscope. High-frequency transient events occur only once, and must be sampled in the same time frame that they occur. If the sample rate isn't fast enough, high-frequency components can "fold down" into a lower frequency, causing aliasing in the display. In addition, real-time sampling is further complicated by the high-speed memory required to store the waveform once it is digitized.
Equivalent-time sampling can be used to accurately acquire signals whose frequency exceeds half the oscilloscope's sample rate. When measuring high-frequency signals, the oscilloscope may not be able to collect enough samples in one sweep. Equivalent time digitizers (samplers) take advantage of the fact that most naturally occurring and man-made events are repetitive. Equivalent-time sampling constructs a picture of a repetitive signal by capturing a little bit of information from each repetition. The waveform slowly builds up like a string of lights, illuminating one-by-one. This allows the oscilloscope to accurately capture signals whose frequency components are much higher than the oscilloscope's sample rate. There are two types of equivalent-time sampling methods: random and sequential. Each one has its advantages. Random equivalent-time digitizers (samplers) utilize an internal clock that runs asynchronously with respect to the input signal and the

signal trigger. Samples are taken continuously, independent of the trigger position, and are displayed based on the time difference between the sample and the trigger. Although samples are taken sequentially in time, they are random with respect to the trigger – hence the name "random" equivalent-time sampling. Sequential equivalent-time sampling provides much greater time resolution and accuracy. It acquires one sample per trigger, independent of the time/div setting, or sweep speed. When a trigger is detected, a sample is taken after a very short, but well-defined, delay. When the next trigger occurs, a small time increment "t" is added to this delay and the digitizer takes another sample. This process is repeated many times, with "t" added to each previous acquisition, until the time window is filled. Sample points appear from left to right in sequence along the waveform when displayed on the oscilloscope screen. Since with sequential sampling the sample is taken after the trigger level is detected, the trigger point cannot be displayed without a variable delay line, which may, in turn, reduce the bandwidth of the instrument. Both require that the input signal be repetitive (Tektronix, 2001).

3. Optical sampling

The optical sampling is a novel method to perform time-resolved measurements of optical data signals at high bit rates with a bandwidth that cannot be reached by conventional photodetectors and oscilloscopes (Schmidt-Langhorst & Weber, 2005). Fig. 1 explains the principle of optical sampling. The upper part of the figure shows an optical data signal with RZ modulation format as example. The data signal is a concatenation of optical data bits, each within a bit slot of 6.25 ps corresponding to a bit rate of 160 Gbit/s. This optical data signal is passed through an optical gate. The gate is closed by default, i.e. it does not transmit the data signal for most of the time except for ultra short periods of time. The period of time for which the gate transmits the data signal is called "gating window". If the width of the gating window is shorter than the bit duration, as shown in Fig. 1, only a fraction of the optical data bit is sliced out. This fraction is called "optical sample". The optical sample is determined by the instantaneous amplitude of the data bit at the sampling time. Ideally, the sampling gate should exhibit a linear transfer function making the amplitude of the optical sample directly proportional to the instantaneous power of the data signal at the sampling time.

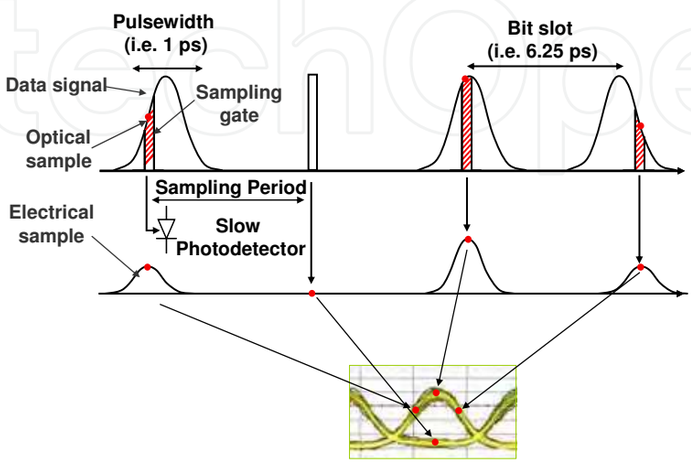


Fig. 1. Operating principle of optical digital sampling

In order to avoid high-speed electronic signal processing for the detection of the optical samples, it is useful to operate the sampling gate with a modest repetition frequency, then only equivalent-time sampling techniques are considered. At the output of the detector, the "electrical sample" appears broadened in time due to the low bandwidth of the detector, but still generates a photocurrent that is proportional to the instantaneous optical power of the optical data bit at the sampling time. After a transimpedance amplifier, the peak voltage V_p of each electrical sample is measured by an ADC. The eye diagram of the optical data signal is obtained from the measured V_p-values if the corresponding sampling times are known.
The optical sampling technique described in Fig. 1 allows to visualize the eye diagram of any data signal that has been encoded by an amplitude modulation format. In the case of a phase modulation format, this sampling technique will not distinguish between logical mark and space levels in the eye diagram. Up to now, only few work has been reported on the monitoring of phase modulated optical data signals. In a simple approach, a phase demodulator was incorporated in an optical sampling system (Schmidt-Langhorst et al., 2005). The demodulator converts the phase modulated data signal into an amplitude modulated data signal before the sampling operation. Another approach is the measurement of constellation diagrams of a phase modulated data signal (Dorrer et al., 2004). Such diagrams represent the amplitude and phase information of the data signal in the complex plane. Moreover FROG technique can be exploited to acquire signal amplitude and phase information.
For sake of shortness we consider here optical sampling techniques for solving only the signal amplitude.

3.1 Sampling gate generation

The generation of the sampling gate is the main subsystem of an optical sampling oscilloscope. It can be performed exploiting nonlinear interactions between the signal to be resolved and an ultra-short pulse train that acts as sampling signal.
The most important parameters of the sampling pulse source are the timing jitter and the pulse width. The timing jitter of the pulse source determines the timing jitter of the whole sampling system, whereas the pulse width limits the temporal resolution of the sampling system. As a rough estimate, a timing jitter of less than 300 fs and a pulse width of about 1 ps are necessary to measure a 160 Gbit/s optical eye diagram. Another important parameter is the repetition frequency of the pulse source. The required sampling rate is typically a few hundred MHz, since the O/E detection frequency in the optical sampling systems is limited to a few hundred MHz.
Different techniques can be considered to generate the sampling signal. Directly modulated, gain-switched laser diodes exhibit high jitter and could require additional compression stage (Ohta et al., 2000). Distributed FeedBack DFB lasers in continuous wave mode cascaded by electroabsorption modulators (EAM) to carve sampling pulses generate broad pulses due to the limited bandwidth of the available EAM's (Otani et al., 1999). Therefore, the pulses had to be compressed for the application as sampling pulses. Hybrid mode-locked semiconductor laser diode offers the potential of monolithic integration but the repetition rate has to be usually reduced using external $LiNbO_3$ amplitude modulator (Schmidt et al., 2002b). Mode-locked Erbium doped fiber lasers are the most widely used sampling pulse sources due to their very low jitter. Also in this case the pulse repetition frequency has to be externally reduced to a few hundred MHz by gating the pulse train with a $LiNbO_3$ modulator (Li et al., 2004; Li et al., 2001; Takara et al., 1996a,b).

The most common techniques used to produce optical nonlinear interaction for the generation of the sampling gate exploit optical fiber, crystals and waveguides or semiconductor devices. A summary of all nonlinear effects used for optical sampling is reported in Tab. 1.

Material	Nonlinear effect
Optical fiber	FWM XPM induced wavelength shifting NOLM Kerr gate
Semiconductor devices	FWM in SOA UNI GT-UNI EAM TPA
Crystals and waveguides	SFG SHF/DFG

Table 1. Summary of nonnlinear effects and nonlinear media exploited for optical sampling.

3.1.1 Optical fiber

The ultra-fast Kerr nonlinearity of the optical fiber provides short gating windows comparable to those of the crystal based gates. The exploited nonlinear processes include four wave mixing (FWM) (Miyazaki & Kubota, 2003), parametric amplification (Li et al., 2001) and cross phase modulation (XPM) induced wavelength shifting (Li et al., 2004). As the efficiency of these processes is rather small, high peak powers were needed for switching. The operational wavelength range of FWM-based all-optical sampling is usually limited by the phase-matching condition. Moreover, in order to cover the whole usable signal wavelength band, the wavelength of the sampling pulses should be set far away from that of the signal, which results in poorer temporal resolution, due to the relatively large walkoff between the signal and sampling pulses. Compared to FWM-based schemes, XPM-based optical sampling can place the sampling pulses just outside the usable signal wavelength region, therefore, the whole usable signal wavelength band can be covered, while the temporal resolution at the order of the sampling pulse width is maintained. However, XPM-based schemes exploiting narrow filtering are more sensitive to the chirp of the data signal, which can introduce some distortions.

Interferometric gates based on highly nonlinear fibers need less peak power of the sampling pulses to achieve gating windows with high on-off contrast. Examples include the nonlinear optical loop mirror (NOLM) (Schmidt et al., 2002a) and the so-called “Kerr gate” (Schmidt-Langhorst et al, 2002). The latter was recently combined with the effect of parametric amplification in (Watanabe et al., 2004).

3.1.2 Crystals and waveguides

For the purpose of obtaining higher sensitivity and higher temporal resolution, some sampling systems employ sum frequency generation (SFG) in the nonlinear crystals (Yamada et al., 2002), periodically poled Lithiumniobate (Yamada et al., 2004; Nogiwa et al., 2000; Ohta et al., 2001) or the organic crystal (Takara et al., 1996b). While these gates provide very short optical gating windows (<1 ps), their main drawback is the required high peak

power, which is necessary to generate a sufficient amplitude of the frequency converted signal. In general, the use of periodically poled material reduces the power requirements as long interaction lengths without loss of phase matching can be achieved. Moreover, if the SFG process is performed with sampling pulses at about 780 nm, the generated light has a wavelength of about 520 nm and can be easily separated from the sampling pulse light as was shown in (Jungerman et al., 2002). In addition to the SFG process, the cascaded $\chi(2)$ processes of second harmonic generation and difference frequency generation (SHG/DFG) have been used as well (Kawanishi et al., 2001).

3.1.3 Nonlinear effects in semiconductor devices

The resonant nonlinearity of a semiconductor optical amplifier (SOA) requires less optical power for the gating pulses (Shirane et al., 2000). Devices based on conventional FWM in SOA's suffer from the fact that the conversion efficiency and the signal-to-background ratio drop rapidly for wavelength detunings between control and data wave larger than some nanometers. So, for the sake of high conversion efficiency or high FWM output power (i.e., high optical power of the FWM signal at the SOA output), the signal has to be kept within the gain wavelength region of the SOA. Hence, the data signal will contribute to gain saturation in the SOA. This is unwanted in sampling applications, where a strict linearity of the FWM output power versus the data input power is required for a quantitative assessment of the shape of the data pulses. Additionally, there is a strong contribution of amplified spontaneous emission (ASE) noise to the converted FWM signal, since the data is within the spectral range of the ASE. A higher switching efficiency is obtained by XPM in an SOA in combination with an interferometric configuration as gate. A promising gate of this kind is the so called "ultrafast nonlinear interferometer" (UNI), which was used in (Kang & Dreyer, 2003). However, this gate suffered from the amplified spontaneous emission (ASE) of the SOA. An EAM with sophisticated synchronization and driving electronics was additionally needed to suppress the ASE after the UNI gate. In a more advanced scheme, the superior gating performance of interferometric optical gates was combined with the so called gain-transparent operation of an SOA. In this operation of the SOA, the wavelength of the data signal is outside the gain spectrum of the SOA. Therefore it does not suffer from ASE degradation. Moreover, the gain-transparent SOA gate exhibits a linear transfer function for the data signal. This is in contrast to the conventional SOA gates, which show a strong saturation. Finally, the gain-transparent operation enables a wide wavelength acceptance range of the gate. The gain-transparent configuration was used in the "gain-transparent ultrafast-nonlinear interferometer" (GT-UNI) sampling gate in (Schmidt et al., 2002b). For the sake of completeness it should be mentioned also that even EAM have been used recently as sampling gates in optical sampling experiments. Since the width of the gating window, which can be achieved with an EAM, is rather large (about 5 ps), these gates could be applied only to bit rates up to 40 Gbit/s (Shake et al., 2003b). Recently though, eye diagrams even at a bit rate of 160 Gbit/s were measured using a double-pass EAM configuration (Kang & Dorrer, 2003).

3.1.4 Two photon absorption (TPA) in semiconductor devices:

The phenomenon of TPA is a nonlinear optical-to-electrical conversion process where two photons are absorbed in the generation of a single electron-hole pair (Folliot, 2002). It occurs when photons of energy E_{ph} are incident on the active area of a semiconductor device with a

bandgap exceeding E_{ph} but less than $2E_{ph}$. The generated photocurrent is proportional to the square of the intensity, and this nonlinear response enables the use of TPA for optical sampling. As TPA is an instantaneous optical nonlinearity, it may be used for all-optical high-speed sampling in photonic systems. The main difficulty with using TPA for high-speed optical sampling is its inherent inefficiency, which means that such systems either require high optical intensities or very long detectors, making them unsuitable for practical telecommunications applications. One possible way to overcome this efficiency problem is to employ a semiconductor microcavity (Krug et al., 2004), which should significantly enhance the TPA response of the device, and enable the implementation of a practical sampling element for high-speed optical systems.

3.2 Optical sampling parameters

An optical sampling system is characterized by the following main parameters:

Temporal resolution

It is typically specified by the full-width at half maximum (FWHM) of the sampling system gating window The temporal resolution is equivalent to the bandwidth of the sampling system.

Timing jitter

The timing jitter is typically specified as root-mean-square (RMS) jitter.

Wavelength range

It is usually specified as 3 dB bandwidth and defines the range of wavelengths, which a data signal can have to be accepted by the sampling system.

Sensitivity

There is no common definition of this parameter with respect to optical sampling systems. Some authors use the product of the average sampling pulse power and the peak signal power. Another definition of the sensitivity uses the peak power of the signal pulses, which is required to achieve a certain displayed signal-to-noise ratio (Yamada et al., 2002) or in case of SFG the well know conversion efficiency parameter.

Dynamic range

It is the power range in which the signal under investigation must fall.

Polarization sensitivity

It describes the amount by which the amplitude of the generated samples varies, when the polarization of the signal under investigation changes.

Applicable bit rate

It is the range of bit rate, at which a particular sampling system was able to display an open eye diagram.

3.3 Synchronous, quasi-synchronous and asynchronous optical sampling

As reported in Fig. 2, in the synchronous sampling configuration, the sampling gate is opened synchronous to the optical data signal but with an increasing time delay in order to scan over the complete bit slot. Thus a technique is needed for the synchronization of the sampling gate to the optical data signal under investigation. This function is performed by an optical clock recovery (CR).

The quasi-synchronous scheme requires an additional subsystem to impose a frequency mismatch between the repetition rates of the signal under test and the sampling signal. In this way a complete scan of long signal time intervals can be directly achieved. In the asynchronous sampling configuration, the clock processing is omitted and the sampling

process is performed at random times. The sampling times are derived from an arrival time measurement of the sampling pulses themselves. As compared to the synchronous sampling configuration, the random sampling configuration requires less components as there is no need for a clock processing circuitry. However, it requires the use of a special O/E-detector, which performs the arrival time measurement of the sampling pulses with high temporal accuracy, as an error in the arrival time measurement directly translates into timing jitter of the sampling system.

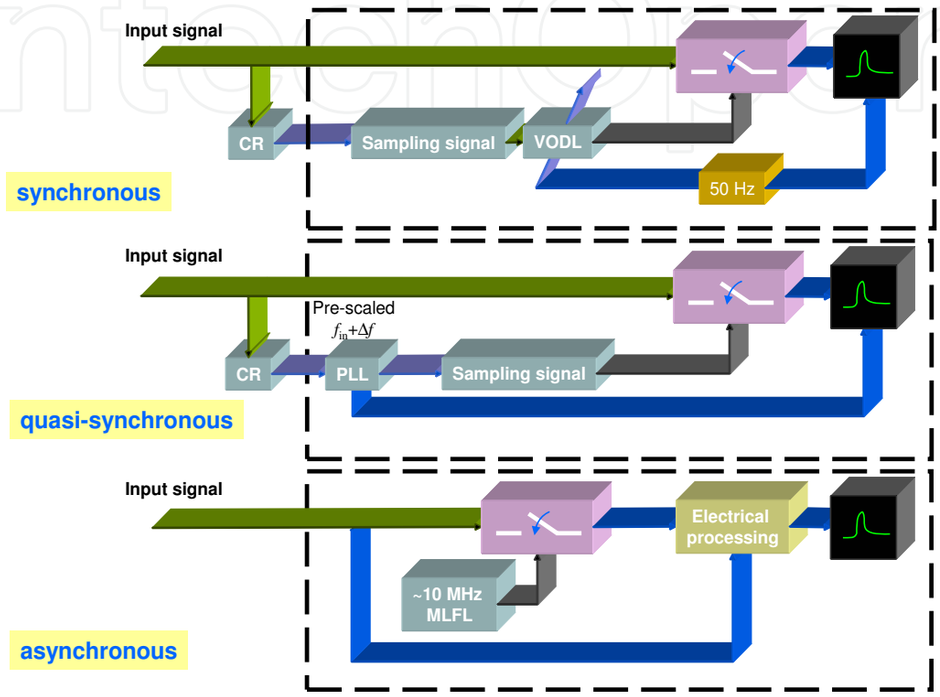


Fig. 2. Scheme of a synchronous (top), quasi-synchronous (center), and asynchronous (bottom) optical digital sampling.

In the following sections the implementation of synchronous, quasi-synchronous and asynchronous optical samplers exploiting optical fiber nonlinearities is presented.

4. Synchronous optical sampler based on Kerr nonlinearities

In the synchronous sampling technique, the sampling signal has to be synchronized with the signal to be sampled, thus requiring some kind of synchronization circuitry. The proposed scheme is based on the nonlinear effects in a highly non linear fibre. The accuracy of this sampling technique strongly depends on the non linear phenomenon efficiency by means of the non linear coefficient, and the fibre length. Nowadays, HNLFs with a flat chromatic dispersion curve and high birefringence are available, thus avoiding efficiency reduction caused by signals walk-off and polarization fluctuations.

The principle of the implemented optical sampler is the same as for commercial electrical sampling oscilloscopes. A schematic about the sampling principle is displayed in Fig. 3. In an ideal sampling, the signal to be measured S(t), is multiplied in the time domain by a delta signal $\delta(t_0)$. The result of the interaction between the two signals, is the power of $S(t)$ measured for $t = t_0$, that is $S(t_0)$. By continuously time shifting the delta signal over $S(t)$, it is

possible to measure the signal power at different instants t_i. Such samples represent a replica for the signal under measure. In Fig. 3(a), the principle scheme about the ideal signal sampling is shown. In a real measurement, the sampling signal will have necessarily a non-zero time duration (Fig. 3(b)); thus consisting in a unavoidable sampling error.

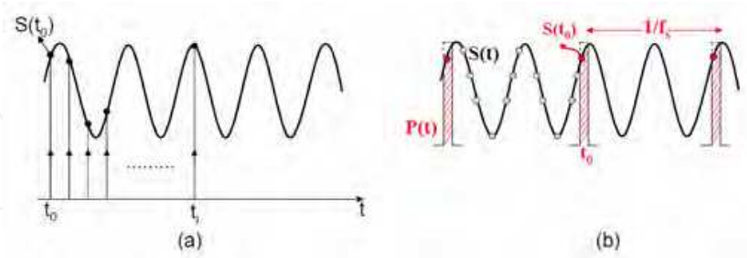


Fig. 3. Ideal operating sampling principle (a), and the real sampling of a periodic signal (b).

If the signal to be sampled is periodic with a period T, it is possible to sample it using another periodic signal whose period T_S is a multiple of T ($T_S = mT$). The accuracy of the sampling process is expressed by:

$$\varepsilon = S(t_0) - f_S \int_0^{1/f_S} S(t)P(t-t_0)dt \tag{4.1}$$

where $P(t)$ is the sampling signal, and f_S is the sampling frequency ($f_S = 1/T_S$). The previous technique, can be implemented exploiting whatever effect between $S(t)$ and $P(t)$, that gives a well known function of the signal power. A non linear effect that can be exploited is the Four Wave Mixing (FWM). The FWM non linear Kerr effect takes place when two or more powerful signals at different wavelength propagate through a non linear medium. When two optical signal $P(t)$ with a wavelength λ_i, and $S(t)$ with a wavelength λ_j, are transmitted through a non linear device, new components (called conjugate components) are generated with wavelengths related to the difference $\Delta\lambda = |\lambda_i - \lambda_j|$. In Fig. 4 it is displayed the FWM effect in the frequency domain. The conjugate component at the wavelength $\lambda_i - \Delta\lambda$ has a power proportional to $S(t)$, and then it can be filtered out and detected, measuring the original signal. The key parameters in this technique are the non linear coefficient g of the used non linear medium, and the power of the signals.

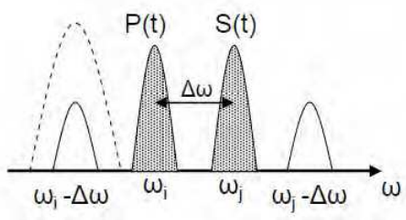


Fig. 4. FWM effect taking place when two powerful signals P(t) and S(t) are launched through a non linear device.

The FWM efficiency is given by:

$$\eta = (\gamma PL)^2 \tag{4.2}$$

where L is the fibre length, and P is the peak power of the sampling signal. The temporal resolution of the fibre based all optical sampler is determined by a combination of the

sampling pulse width, and the temporal walk-off due to the chromatic dispersion between the sampling pulses and the signal during the sampling process. Afterwards, in order to obtain a good resolution, it is necessary to sample the signal with short sampling pulses, and to have a low value of dispersion slope. In a first implementation of the sampler, a fibre based active mode locking source has been used in order to generate the sampling pulses, with a repetition frequency of 10 GHz and a pulse width of about 4 ps. The laser source output has been directly used to sample a nonreturn-to-zero (NRZ) modulated signal. As further measure, a return to zero (RZ) signal was sampled, verifying the time resolution of the scheme. For the RZ signal sampling, a higher time resolution was obtained compressing the ML source pulses down to about 1 ps, and using that as sampling signal. For both the measures, the FWM component generated during the transmission was filtered out by means of an optical filter (dotted line in Fig. 4).

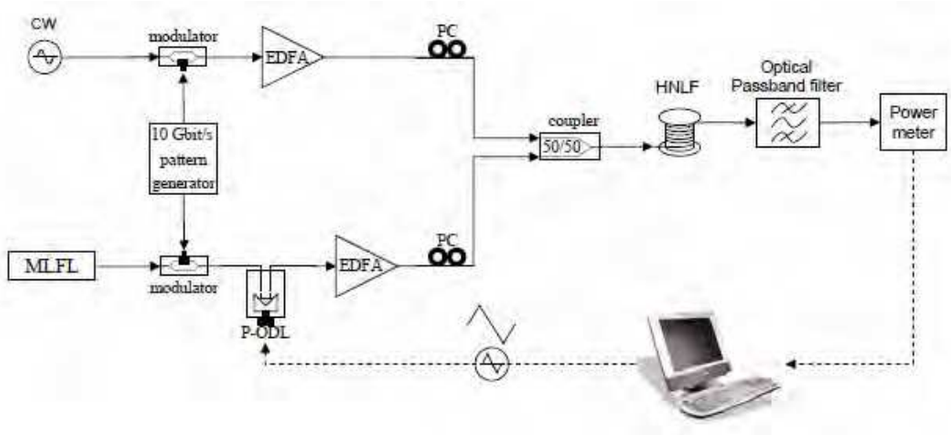


Fig. 5. Setup of the implemented synchronous optical sampler.

In Fig. 5, the setup of the implemented synchronous optical sampler is shown. In order to validate the functioning of the scheme, a NRZ signal, obtained modulating a 1550 nm Continuous Wave (CW), was sampled. For the experiment, a 400 m long HNLF with $\gamma = 10W^{-1}Km^{-1}$ and slope $S = 0.3\ ps/nm^2/Km$, was used as non linear medium. The NRZ signal was coupled together with the ML laser source output, whose wavelength was $\lambda_s = 1557$ nm. The power and the polarization state of both signal and pump (sampling signal) was optimized by means of Erbium Doped Optical Amplifiers and polarization controllers respectively. A Piezo-electric Optical Delay Line (P-ODL) driven by a 100 MHz electric triangular waveform, was used in order to shift the sampling pulses with respect to the signal. In such a way it is possible to visualize the behaviour of the mean power at the output of the optical filter with a refreshing time of the order of 100 ms. A 150 MHz photodiode (PD) and a 500 MHz oscilloscope triggered with the 100 MHz triangular waveform, was used to display the sampling result. An alternate modulation pattern was used, whereas the sampling signal frequency was fixed to 5 GHz in order to have the same periodicity as the signal under test. The mean power measured by changing the sampling pulses time position, directly gives the NRZ signal shape. In Figure 6 the results about the sampling of the NRZ signal are reported. The signal was opportunely pre-distorted in order to evaluate the sampler accuracy. In order to demonstrate the high resolution that can be obtained exploiting the Kerr non linearities (i.e. FWM), the ML laser source pulses was resolved. In this measure, the setup was slightly different from the scheme of Fig. 5. In

particular, the ML pulsed signal was split, compressed and used also to generate the sampling signal. The compression was made by means of a higher order soliton compressor, obtaining pulses of about 350 fs. In Fig. 7 the scheme of the compressor and the obtained compressed optical pulse autocorrelation trace are displayed.

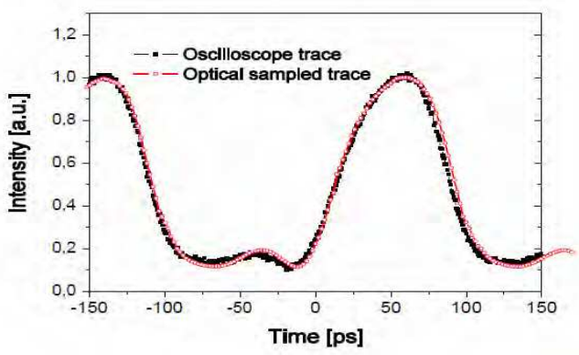


Fig. 6. comparison between the implemented optical sampler and the commercial oscilloscope measures.

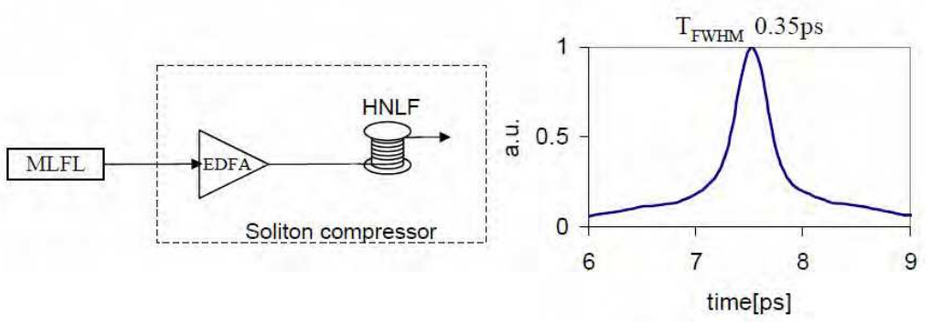


Fig. 7. Scheme of the higher order soliton compressor (left), and autocorrelation trace of the obtained compressed pulse (right).

In Fig. 8, the 10 GHz ML sampled pulses (left) and the comparison between the autocorrelation trace measured by means of a commercial autocorrelator (right) are reported.

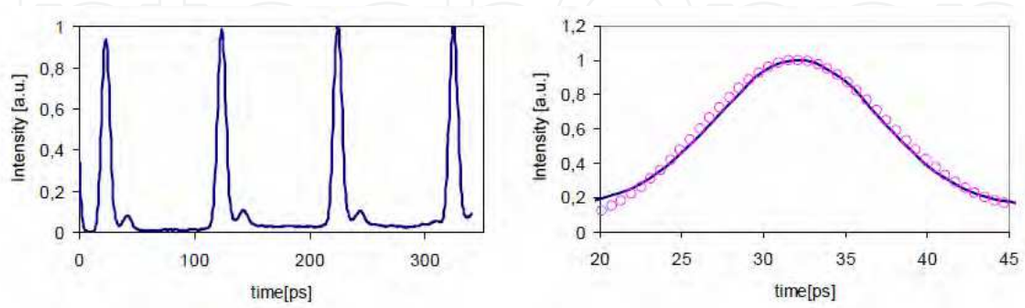


Fig. 8. 10 GHz sampled signal (left), and comparison between the autocorrelation traces (right).

Another experiment was made in order to evaluate the sampler resolution. The signal to be measured was obtained time-multiplying the ML laser source output with an all optical

multiplexer realized with the split-and-delay technique. In Fig. 9 are reported the results of the 80 GHz signal sampling.
Finally, in order to qualitatively estimate the maximum resolution of the implemented optical sampler, the signal to be sampled was distorted changing the power level in the compressor, obtaining an asymmetric and irregular optical pulse. This way, sub-picosecond dynamics was obtained and measured by the sampler, verifying its functioning for the measure of ultra short signals. In Fig. 10 the result about the sampling of the distorted pulse is shown.

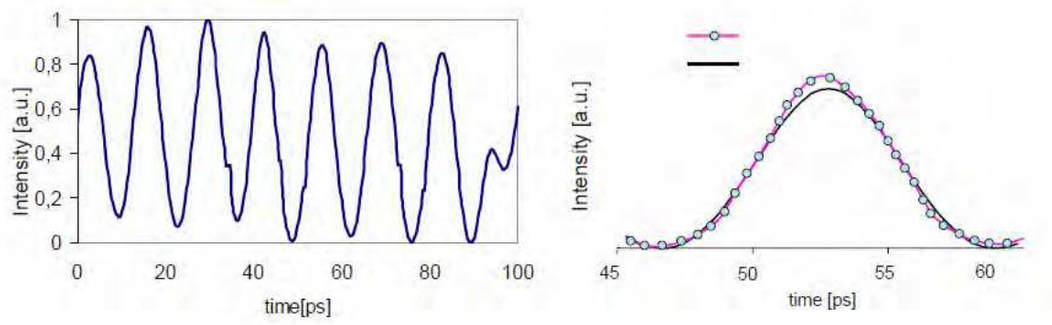


Fig. 9. 80 GHz sampled signal (left), and comparison between the autocorrelation traces (right).

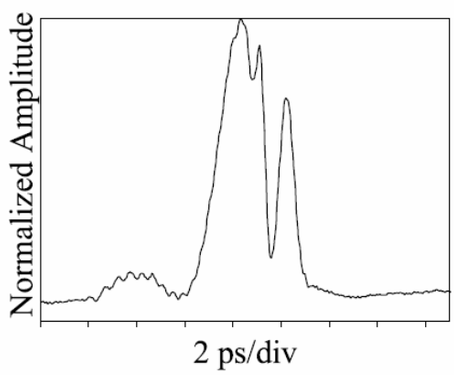


Fig. 10. Intensity trace of the distorted sampled pulse.

A scheme similar to the one described was implemented exploiting the non linear effect of cross phase modulation (XPM). In particular, the exploited effect was the XPM-induced polarization rotation. In Fig. 11 the setup of the optical sampler is reported. As in the previous scheme, an ultra short pump with high peak power interacts with the signal while propagating in the non linear fibre. In this optical sampler, a quasi instantaneous phase rotation (typical response time < 50 fs) is induced by the sampling pulse on the signal portion superimposed to the pump.
By means of a polarization controller and a polarizer at the output of the non linear element, it is possible to extract the portion of the signal time overlapped to the pump. This power portion can be then measured by using a narrow bandwidth photoreceiver. If the pump is short enough, that measured power can be approximated with the instantaneous signal power. As described before, by shifting the pump with respect to the signal its time shape

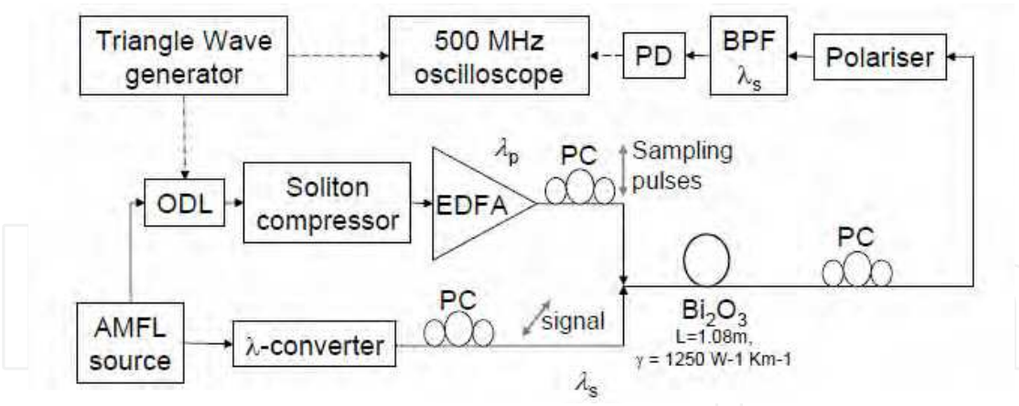


Fig. 11. Experimental setup of the synchronous sampler based on XPM-induced polarization rotation in 1 m of Bi_2O_3 fibre.

can be measured. One difference with respect to the previous scheme, is that in this case, the non linear medium is a Bismuth Oxide fibre (Bi_2O_3) with a very high non linear coefficient γ= 1250 $W^{-1}Km^{-1}$, a total attenuation a = 6 dB and an accumulated chromatic dispersion D_t = - 0.33 ps/nm at a wavelength λ = 1550 nm. Such a high non liner coefficient permits to strongly decrease the fibre length down to L = 1.08 m. The use of short fibre spans reduces at the same time the polarization fluctuation and the scheme footprint, making the system more stable and compact. The sampling pulses was obtained by means of soliton compression on the ML sources and the signal under test was obtained by λ-converting the same ML laser. The wavelength conversion was made exploiting FWM in 250 m of HNLF. Moreover, the signal was coupled with the pump with a 45°-rotated polarization state in order to obtain maximum XPM-induced polarization rotation. Fig. 12 (left) shows the optically sampled pulse shape, whose pulse width of 6 ps was measured. In order to verify the accuracy of the implemented scheme, the obtained sampled trace autocorrelation was compared with the results supplied by a commercial autocorrelator obtaining a very good agreement between the traces, and verifying a picosecond resolution of the sampler (see Fig. 12 (right)).

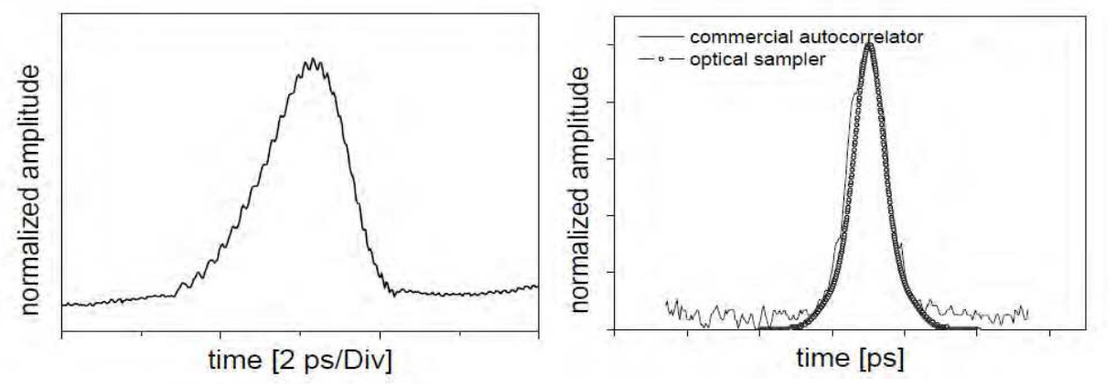


Fig. 12. 6 ps soliton pulse measured by the optical sampler (left) and comparison between the autocorrelation traces supplied by a commercial autocorrelator and the processed data measured by the implemented optical sampler (right).

5. Asynchronous optical sampling

An important issue of synchronous sampling technique is that it requires a synchronization between the sampling signal and the signal under investigation. Unfortunately, the synchronization of fast optical signals it is not easy and it requires complex all optical techniques and fast electronics. For this reason, it is useful an asynchronous sampling operation. An Asynchronous all optical Sampling Oscilloscope based on FWM in HNLF (ASOF) has been also implemented. The asynchronous solution, based on the knowledge of the mean frequency of the signal under test, avoids the use of a clock recovery circuit, with strong advantages in terms of complexity and cost. This kind of sampler has not only the advantage of not requiring synchronization circuits, but also the capability of describing both signal eye diagram and long bit sequences (several ns), thanks to the asynchronous operation. Moreover, a sub-ps resolution can be obtained due to the exploited ultra fast non linear Kerr effects in fiber. A short refresh time was obtained using a commercial oscilloscope able to directly acquire and process a large amount of data. The working principle of the implemented asynchronous sampler is shown in Fig. 13. As in the previous schemes, the asynchronous optical sampling oscilloscope exploits the non linear interaction between the signal under test and the sampling signal. The signal under test was periodic with a frequency $f_S = 1/T_S$, where T_S is its period.

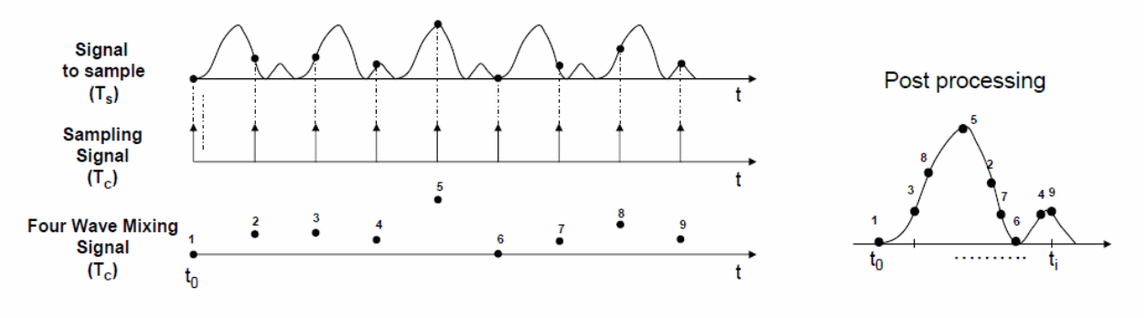


Fig. 13. ASOF working principle.

The sampling frequency f_C is not correlated to f_S, meaning that there is no need for any fixed relation between the two frequencies. Every pulse of the sampling signal generates a pulsed FWM component, whose energy is proportional to the instantaneous power of the signal under test in the corresponding interaction time. Since the frequencies of the involved signals are not correlated, two consecutive samples do not correspond to two consecutive instantaneous power values of the signal; on the opposite the temporal sequence of the samples appears as shuffled sampling of the analyzed signal. Besides, the sample sequence can be stored through an acquisition board, and then the sampled signal can be correctly reconstructed, if the difference of the period T_S - T_C is known. Therefore a post processing can be applied to the sample sequence for re-ordering the collected points and reconstructing the original signal shape. In more details, the position of the *i-th* sample, with respect to the period of the signal under test, is defined by the following equation:

$$t_i = t_0 + Mod\left[i\frac{(T_S - T_C)}{T_S} \right] \tag{5.1}$$

where t_0 is a reference initial time that can be set to zero. The samples can not be equally spaced depending on the relationship between T_S and T_C, and on the acquisition time. Consequently a mean resolution R of the ASOF can be defined as:

$$R = \frac{T}{N} \tag{5.2}$$

where T is the signal time interval to be resolved, and N is the number of acquired samples. One of the most critical issue of an asynchronous sampling technique is the phase noise that can be introduced by the sampling process. For this reason an analytical study of the phase noise generated in the implemented scheme was made. Due to the asynchronous behavior of the sampling operation, the introduced phase noise strongly depends on the phase noise of the signal under test and of the sampling pulse train. For the implemented scheme, it is possible to neglect the phase noise of the sampling pulse since its value was verified to be one order of magnitude lower than the phase noise of the considered signal. The analysis was made considering a sinusoidal waveform at 39.9 GHz as signal to be resolved. In this case, being $S(t)$ the signal under test, it can be modelled in the time domain as the sum of two components: the first one represents the noise-free sinusoidal signal $S_{nf}(t)$, and the second one $H(t)$ includes all amplitude and phase noise contributions:

$$S(t) = S_{nf}(t) + H(t) \tag{5.3}$$

Considering the signal electrical spectrum $P(f)$, the noise term can be modelled as the sum of the sinusoidal functions that represent all the components of the sideband noise of $P(f)$:

$$H(t) = \sum_{i=0}^{M} a_i \sin(2\pi(f_{low} + i\Delta f) + \delta i) \tag{5.4}$$

where the sideband noise of the electrical spectrum has been divided in M slices with a frequency step equal to Δ_f , while f_{low} *and* $f_{high} = (f_{low}+M\Delta f)$ are the upper and lower bounds of the noise bandwidth to be considered; a_i is the spectral power associated to the frequency $f_i = (f_0+f_{low}+i\Delta f)$ being f_0 the carrier frequency of the signal, and δi is a random variable uniformly distributed in the range $0 \div 2\pi$ accounting for the phase of the noise spectral components. The bandwidth $f_{high} - f_{low}$, depends on the time needed for the acquisition of all the optical samples allowing the desired resolution of the signal under test. In the implemented scheme, all the acquisition times are shorter than 10 ms and consequently it is possible to neglect all the noise components at frequencies lower than f_{low} = 10 KHz. The upper limit of the bandwidth to be considered was fixed to f_{high} = 1 MHz, since all higher spectral components present negligible amplitude. $H(t)$ includes both amplitude and phase noise, but it can be demonstrated (Von der Linde, 1986), that for $f_{low} \geq 10$ KHz the phase noise is dominant. Consequently all the contribution of $H(t)$ can be assumed as phase noise, thus making a worst case approximation. The phase noise can be estimated in terms of timing jitter. The jitter can be extracted from the sideband noise of the signal electrical spectrum according to:

$$J\left[f_{low}, f_{high}\right] = \frac{1}{2\pi f_0}\sqrt{\frac{P_{sb}}{P_C}} \tag{5.5}$$

where P_C is the mean power of the sinusoidal waveform $S_{nf}(t)$, and P_{sb} in the integral of the sideband of the electrical spectrum of $S(t)$:

$$P_{sb} = \int_{f_0+f_{low}}^{f_0+f_{high}} \frac{P(f)}{1.2B} df \tag{5.6}$$

As explained in the previous chapter, the factor 1.2 normalizes the filter response of the electrical spectrum analyzer to a rectangular function, and B is the resolution bandwidth of the electrical spectrum analyzer. In the analytical investigation, $H(t)$ was obtained from the experimental sideband noise of the electrical spectrum reported in Fig. 14 (left), concerning a sinusoidal clock at 39.9 GHz.

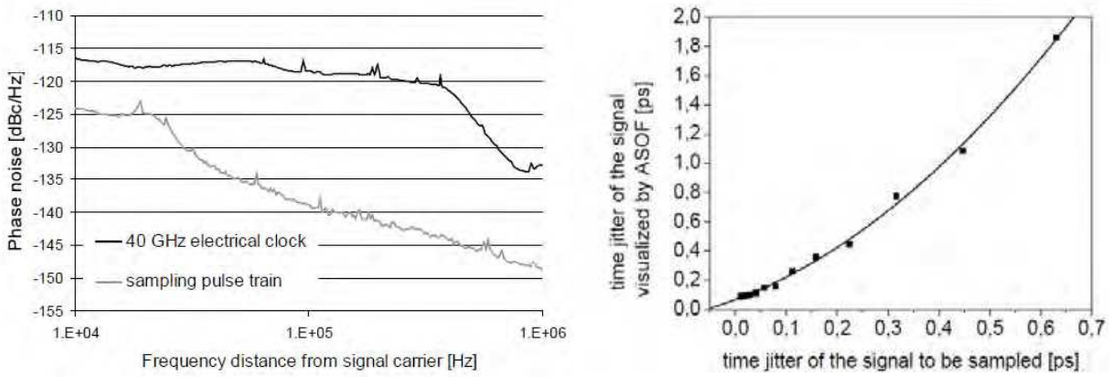


Fig. 14. Frequency distance from signal carrier (left) and analytical time jitter of the sampled signal as a function of the time jitter of the signal to be sampled (right).

The timing jitter of this signal, measured in the range 10 KHz ÷ 1 MHz, is equal to 70 fs. The sampling signal was considered to be a train of ideal delta functions with a repetition rate of 500 MHz, the acquisition time was set to 1 ms, and the time interval to be measured was fixed to 25 ps. The mean resolution can be estimated to be R = 50 fs. An analytical tool extracts the sequence of the instantaneous powers of the signal $S(t)$ corresponding to the interaction times between the signal and the delta function train. The tool then calculates the correct time position for each sample, with respect to the period of the signal to be measured, exploiting eq. 5.1. The timing jitter of the signal measured by the asynchronous sampling operation, could not be evaluated exploiting the previous equations since it was obtained by a data post processing, and its electrical spectrum was not available. Therefore the timing jitter was evaluated directly in the time domain, as it is for any commercial oscilloscope, considering the sampled curve as the sum of an ideal curve and a random variable with a gaussian time distribution. The timing jitter was then measured as the standard deviation of this time distribution, evaluated at half maximum of the curve displayed by the optical sampler. For the implemented scheme, a signal timing jitter of 156 fs was estimated, about two times higher then the timing jitter of the signal under test (76 fs). Consequently, it is possible to assert that the phase noise introduced by the asynchronous sampling operation does not compromise the measure of this 40 GHz signal with a sub-ps resolution. In Fig. 14 (right) the estimated timing jitter of the signal as visualized by the ASOF is plotted as a function of the timing jitter of the signal under test, obtaining a clear parabolic behavior. The increasing timing jitter of the signal to be sampled,

was obtained considering in all cases the sideband noise of the electrical spectrum reported in Fig. 14(left), but with a decreasing mean power P_C of $S(t)$. For an input signal with a timing jitter lower than 100 fs in the range 10 KHz÷1 MHz, the implemented asynchronous sampler allows to describe the signal time evolution with a timing jitter lower than 200 fs. For higher values up to 600 fs, the timing jitter of the sampled curve as displayed by the ASOF does not exceed a value of 2 ps. Therefore this analysis has verified that the asynchronous sampling technique, despite avoiding the clock recovery operation, introduces a low amount of additional phase noise, allowing to measure ultra fast signal with high accuracy. The experimental setup for the ASOF implementation is shown in Fig. 15.

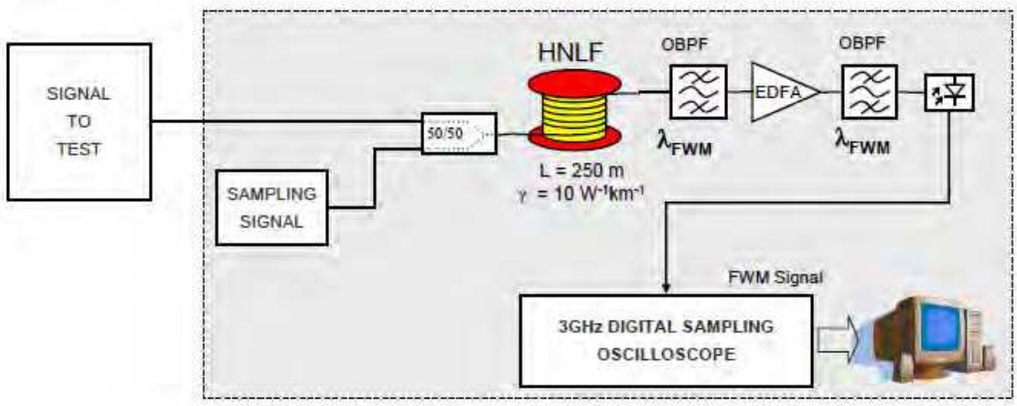


Fig. 15. ASOF experimental setup.

In order to generate the sampling signal, a 10 GHz active ML laser source was exploited, producing sub-ps pulses at a tunable wavelength λ_C. The pulse train repetition rate was then reduced down to 500 MHz by a Mach Zehnder (MZ) intensity modulator. The choice of the sampling rate depends on many factors: the upper value is limited by the bandwidths of the receiver and the electrical oscilloscope used for the acquisition of all the samples. On the other hand, low sampling rates, increase the acquisition time needed to obtain a fixed number of samples, and then require a higher memory capacity in the acquisition board. A sampling rate equal to 500 MHz represented the best trade off, using a 1 GHz receiver and an acquisition board with a memory capacity of 10 MPoints at a rate of 10 GSample/s. The sampling pulses were coupled with the signal under test in a 250 m long span of HNLF (with $\gamma = 10W^{-1}Km^{-1}$) generating the FWM components. An optical tunable filter was then used to extract the FWM components spectrally closer to λ_C thus obtaining a sample power linearly dependent on the instantaneous power of the signal under test. The optical samples were then detected through a 1 GHz bandwidth photo-receiver and measured on a 3 GHz bandwidth oscilloscope working at 10 Gsample/s. The oscilloscope used for the experiment was able to directly acquire and process the data exploiting MatLab scripts. The implemented sampler has the capability to analyze a signal for very long time intervals with high resolution and low refresh time. Considering the measure of a 10 ns long time interval with a desired resolution of 1 ps, the corresponding refresh frequency is about 1 Hz. The accuracy of the sampling technique, depends on the stability of the frequencies f_S and f_C whose mean values have to be measured and used as parameters in the data post processing. As described before, the phase noise was considered in the range

10 KHz÷1 MHz. The lower limit was due to the acquisition time (lower than 10 ms) and assuming that the mean frequency values, which are measured at each acquisition, are not affected by noise components lower than 10 KHz. On the other hand the phase noise components higher than 1 MHz present negligible amplitude and then can be neglected. The resolution of the ASOF is determined by the difference T_S - T_C, by the maximum number of acquired samples, and by the length of the analyzed time interval. According to eq. 5.1, the possibility to finely change the period of the sampling signal allows to significantly modify the sampling resolution. For this purpose, The ML source was provided with a variable optical delay line into the cavity, in order to vary the length of the fibre ring, thus finely changing the repetition rate of the generated sampling pulse train in the range 500 MHz÷1.5 MHz. The previous analytical investigation about the sampler phase noise was validated sampling a Continuous Wave (CW) signal modulated with an electrical 39.9 GHz sine. The sideband phase noise of the electrical spectrum of the clock is reported in Fig. 14 (left) and compared with the curve related to the sampling signal in the range of interest. The corresponding clock timing jitter, measured according to eq. 5.5, was 70 fs, considerably higher than the 5 fs timing jitter of the ML source used as sampling signal. This comparison justifies the assumption of neglecting the phase noise of the sampling signal in the analytical investigation. In Fig. 16 the curve of the optical sinusoidal waveform as measured through the analytical tool and as visualized by the implemented sampler.
In both analytical and experimental cases, the acquisition time was 1 ms and the resolution of 50 fs. The timing jitter, directly measured in the time domain, as described before, was 156 fs and 188 fs in the analytical and experimental cases respectively. In the analytical case, the sampling signal was an ideal delta function train and the amplitude noise, due to the FWM generation, was not considered. Consequently, the comparison in terms of timing jitter of the resolved curve, shows a good agreement between analysis and experiment, confirming the accuracy of the proposed analytical investigation. The potentialities of the ASOF, has been investigated considering a 40 Gbit/s optical NRZ signal. In this case, the optical CW was modulated through the Mach Zehnder modulator driven by a 40 Gbit/s data sequence supplied by a pattern generator.

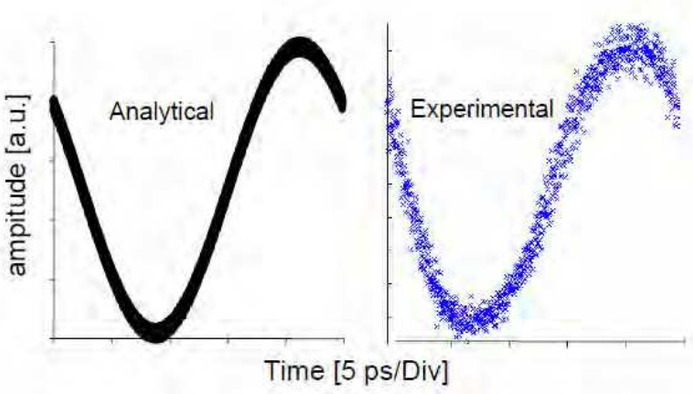


Fig. 16. 40 GHz optical sinusoidal waveform analytically and experimentally sampled.

The electrical clock, as in the previous case, was the 39.9 GHz sinusoidal waveform, whose sideband noise is reported in Fig. 14 (left). In this experiment, the acquisition time was 2 ms. Fig. 17 shows a 32 bit-long sequence (top) and its relative eye-diagram (center), of a signal as visualized by the proposed scheme (right) and by a commercial oscilloscope with a

bandwidth of 53 GHz (left). The same comparison is reported also for the eye-diagram modulating the signal with a (2^{31} - 1)-long Pseudo Random Bit Sequence (PRBS) (bottom). In the case of the 32 bit sequence, the time interval to be resolved was 800 ps and consequently the mean resolution of the ASOF, was 0.8 ps. The comparison demonstrates the higher resolution obtained with the ASOF, that can better resolve the isolated ones and zeroes. The slight increase of the amplitude noise on the mark level in the ASOF traces, was mainly due to the FWM term generation and amplification. For both the 32 bit sequence and the PRBS, the higher resolution of the ASOF, allowed to obtain a good eye opening, especially close to bit transitions. The suitability of the ASOF, to measure ultra fast signals in the whole C-band, has been also demonstrated. Depending on the signal wavelength, the sampling pulse train wavelength can be moved in different spectral regions, in order to optimize the FWM generation.

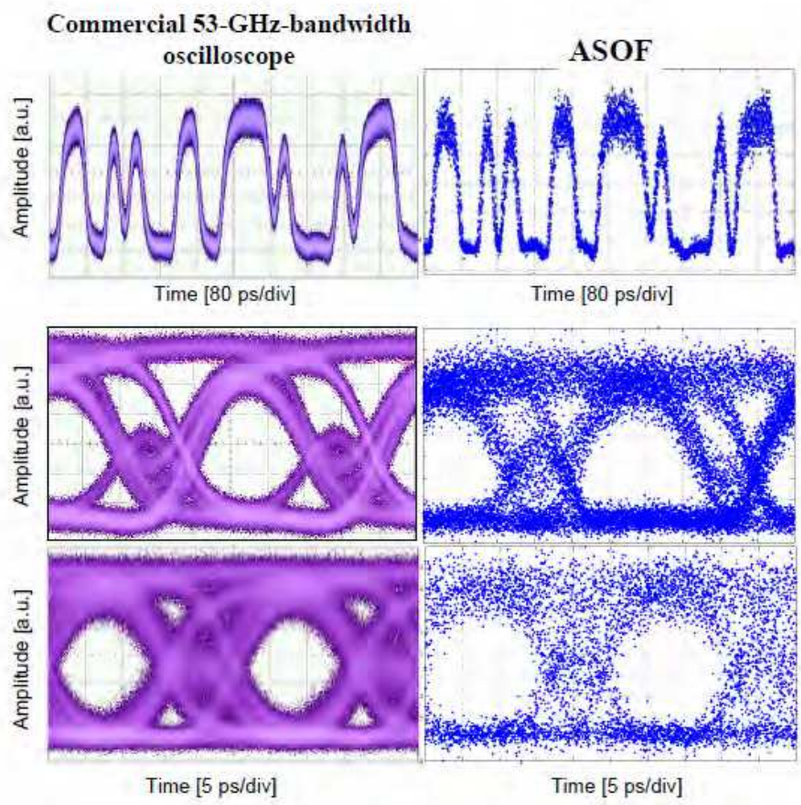


Fig. 17. 40 Gbit/s NRZ signal, visualized by a 53 GHz commercial oscilloscope (left) and by the ASOF (right); Bottom: eye-diagram of a (2^{31} - 1)-long PRBS. The wavelength of the signal under test was 1561 nm, while λ_C = 1552.5 nm.

The tunability of the pulse train source has been obtained inserting into the ML cavity, a tunable optical filter. The main specifications of the laser, such as the pulsewidth and the time jitter, were independent on the selected wavelength in the whole C-band. Fig. 18 (left) shows the optical spectrum at the output of the HNLF for three different wavelengths of the 40 Gbit/s signal under test: 1544 nm, 1556 nm, and 1561 nm. In all cases, the pulse train wavelength was fixed at 1553 nm, corresponding to 9 nm, 3 nm, and 8 nm signal detuning respectively. The same 32 bit-long sequence in the three different cases is reported in

Fig. 18 (right). It can be noticed that the quality of the resolved curves is comparable, making the proposed scheme suitable for applications in the whole C-band. Moreover, the detuning between the signal under test and the sampling pulse train was not a big issue for the FWM generation, for signal spacing up to 9 nm. This value allows to process also ultra fast signals with many frequency components.

As last measure, the high resolution of the ASOF, was demonstrated characterizing the optical pulse generated by a second 10 GHz ML source at 1561 nm. In Fig. 19, the generated optical pulse resolved by the ASOF, is reported. In this case, the timing jitter of the input signal in the range 10 KHz÷1 MHz, was 10 fs. The acquisition time was 800 ns, and the time span was 100 ps; consequently, the mean resolution was equal to about 0.25 ps. The measured 3 dB pulsewidth was 4.2 ps, very close to the value of 4 ps given by a commercial autocorrelator. The accuracy in the sampling of this short pulse, confirmed the high performance of the proposed ASOF measuring signals with bandwidth up to 1 THz.

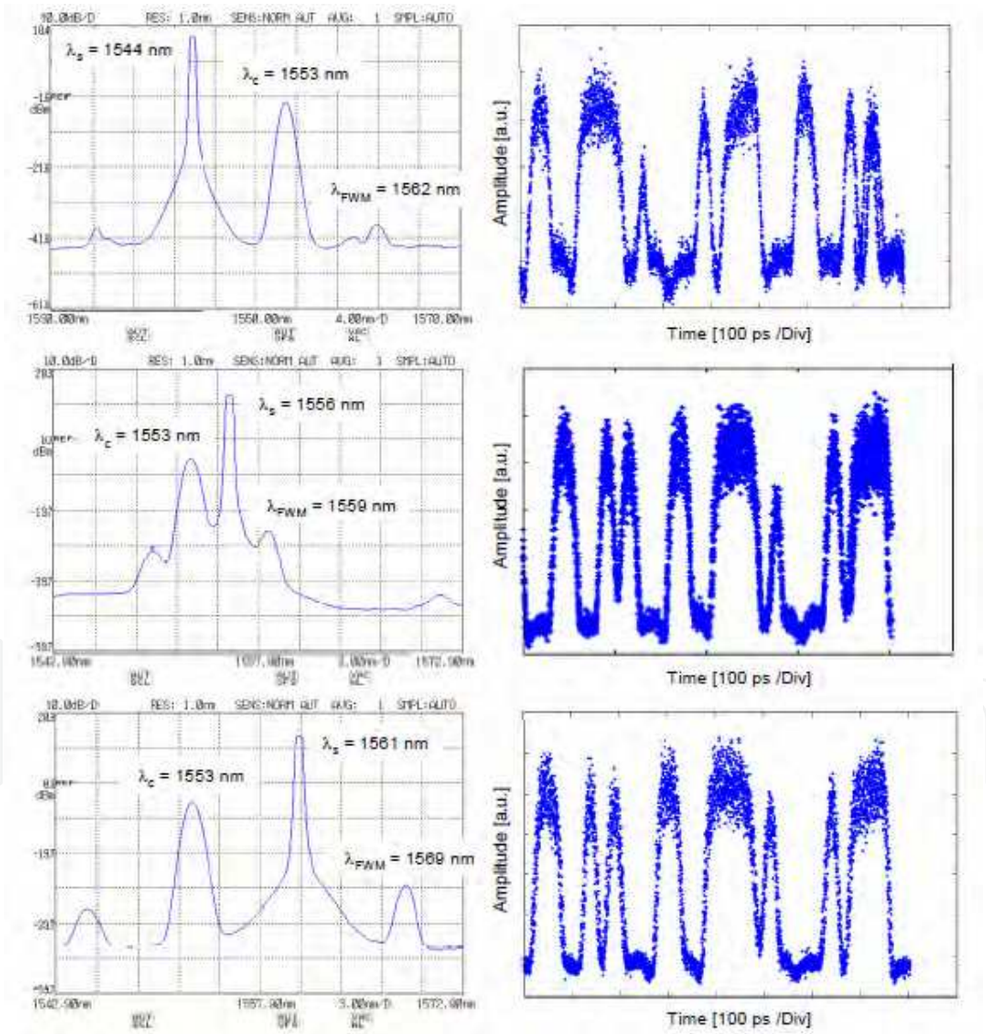


Fig. 18. Optical spectrum at the output of the HNLF (left) and corresponding 32 bit-long sequence resolved by the ASOF (right) in the case of signal wavelength equal to 1544 nm (top), 1556 nm (center), and 1561 nm (bottom).

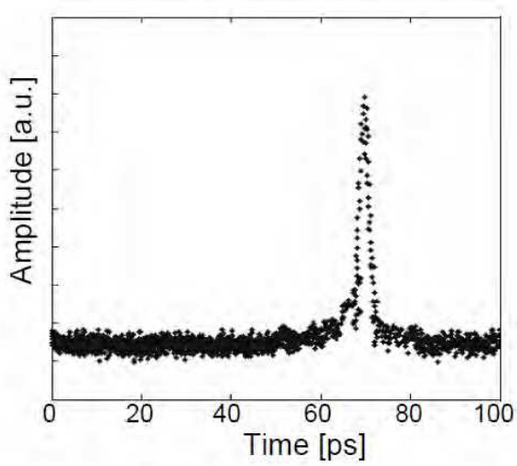


Fig. 19. trace of a 4 ps optical pulse generated by a 10 GHz ML laser source, as resolved by the ASOF.

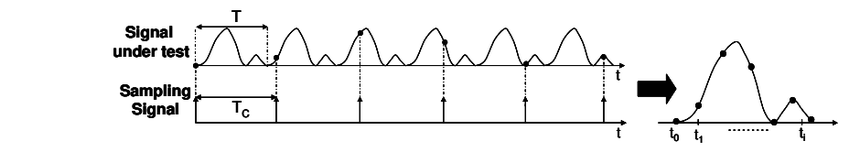
6. Quasi-Synchronous optical sampler

As shown in the previous sections, synchronous sampling methods can typically reach sub-picosecond resolution, but they are able to analyze limited time intervals allowing to resolve only the eye-diagram of a data signal. Asynchronous optical sampling methods can describe long time intervals (> 1 ms), but with longer refresh time due to data post-processing. Moreover they introduce a higher jitter, intrinsic in the asynchronous operation. A possibility to obtain the advantages of both synchronous and asynchronous solutions is to exploit quasi-synchronous sampling (QS). In particular, the implemented sampler was based on the effect of Four Wave Mixing in high non linear fiber. It exploits the nonlinear interaction between the signal to be resolved and a sampling ultra-short pulse train whose frequencies are locked to a fixed difference. With this solution long bit sequences and eye-diagram for a 640 Gb/s data-frame can be displayed without the need of data post-processing and consequently with a very low refresh time (< 1.6 ms), exploiting low-bandwidth electronics. A double PLL scheme able to maintain a fixed frequency mismatch is described. Finally, sub-ps-resolution has been demonstrated by comparisons with a commercial autocorrelator.

The working principle and the setup of the QS optical sampling oscilloscope are shown in Fig. 20 (a,b). The sampling signal is an ultra-short pulse train at low repetition rate; when a frequency mismatch is imposed between the repetition rates of the signal under test and the sampling signal, a shift of the sampling signal on the signal under test is induced, as shown in Fig. 20(a). If the signal under test is periodic with $T=NT_s$ (being T_s the bit time) and N the sequence bit number, the period of the sampling signal can be chosen as $T_C = NT_s + \Delta t$, where Δt is the desired temporal resolution. This way samples are collected consecutively, and no post processing is required. Due to the low repetition rate, it is possible to reconstruct the sampled signal using a slow PhotoDiode and a low-bandwidth oscilloscope, acquiring just the samples sequence envelope. A piezoelectric delay line inside the optical sampling source cavity makes the source acting as an Optical VCO (OVCO), allowing to finely tune the sampling frequency f_C. Through a double PLL scheme, the difference

between the N^{th} sub-multiple of the signal frequency f_S and the sampling frequency f_C ($f_{LO}=f_S/N-f_C$) is maintained constant. The frequency mismatch is imposed using a local oscillator and is determined by the desired resolution, according to the formula reported in Fig. 20(a). Therefore, it is possible to tune the desired resolution Δt just changing the value f_{LO}. Furthermore, exploiting a wavelength-tunable sampling signal, we obtain a QS sampler working within whole C-band. If N=128, every bit pattern with a period of 2^n bit and n ≤ 7 can be resolved. For example, when f_S = 10 GHz, choosing a sampling signal repetition rate f_C = 78.124 MHz and a frequency mismatch f_{LO} ~ 600 Hz, a 100 fs temporal resolution can be reached. This solution provides a refresh time of ~ 1.6 ms. At last, tuning the sampling signal repetition rate, it is possible to resolve also bit pattern with a standard length of 2^{n-1} bit.

The optical sampler exploits the FWM nonlinear interaction between the signal under test and the sampling signal (that acts as a pump). The two optical signals are coupled together and launched into a Highly Nonlinear Fiber (HNLF). The FWM-generated signal corresponds to the sequence of samples. The FWM effect is maximized by means of Automatic Polarization Controllers (APC) that polarization align the two signals. An optical BPF (Band-Pass Filter) centred at the FWM wavelength is used to isolate the samples. Each APC includes an electro-optical feedback, making the scheme polarization insensitive.



(a)

$$f_{LO} = \frac{\Delta t / N \cdot f_s^2}{N + \Delta t \cdot f_s} \cong \Delta t / N^2 \cdot f_s^2 \qquad N >> \Delta t \cdot f_s$$

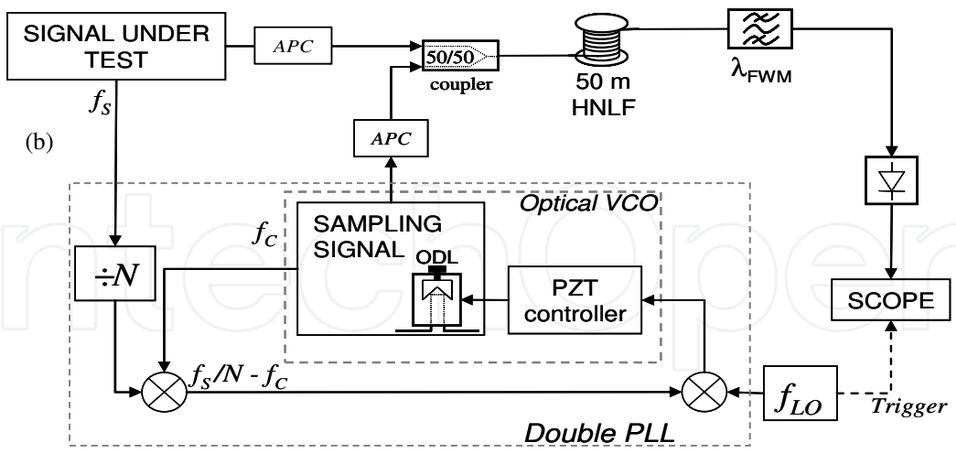


Fig. 20. Working principle of quasi-asynchronous sampling operation and Schematic of the quasi-asynchronous sampling oscilloscope.

Experimental measurements have been carried out using a 640 Gb/s RZ signal as signal under test. Such signal has been obtained time-multiplexing a RZ 10 Gbit/s one (4x10 Gb/s channels spaced 1.56 ps each other), produced by a 10 GHz Actively Mode-Locked Fiber Laser (AMLFL) and modulated by a Mach Zehnder modulator with a N = 8 bit pattern. A

pulse compression stage is required to reduce the pulsewidth from the original 4 ps of the AMLFL down to 550 fs. The sampling signal is obtained with a second AMLFL acting as an OVCO, followed by a compression stage to reach a pulsewidth of 500 fs. A Δt of 50 fs is imposed setting a frequency mismatch f_{LO} = 80 KHz. The sampling pulses are then coupled with the signal under test into 50 m of HNLF. The average power of the sampling signal and the signal under test was 11 dBm and 9 dBm respectively. The wavelengths of the two signals have been set at 12 nm distance (λ_S=1560 nm, λ_C=1548 nm) due to their large bandwidth; the FWM signal generated at 1536 nm is filtered by a 1.2 nm BPF, then the sampled signal is photo-detected and viewed on a 600 MHz real-time oscilloscope. When the oscilloscope is directly triggered by f_{LO} the bit pattern is visualized (Fig. 21 (a)), while eye diagram evaluation can be performed using a xN frequency multiplier at the trigger (Fig. 21 (b)). To confirm the accuracy of the acquired trace, a comparison between the autocorrelation supplied by a commercial autocorrelator and the one measured from the optical sampler trace has been carried out (Fig. 21 (c)). The good agreement between the two traces confirms the effectiveness of the sampler in terms of shape and pulsewidth measurement; the measured pulsewidth is 550 fs.

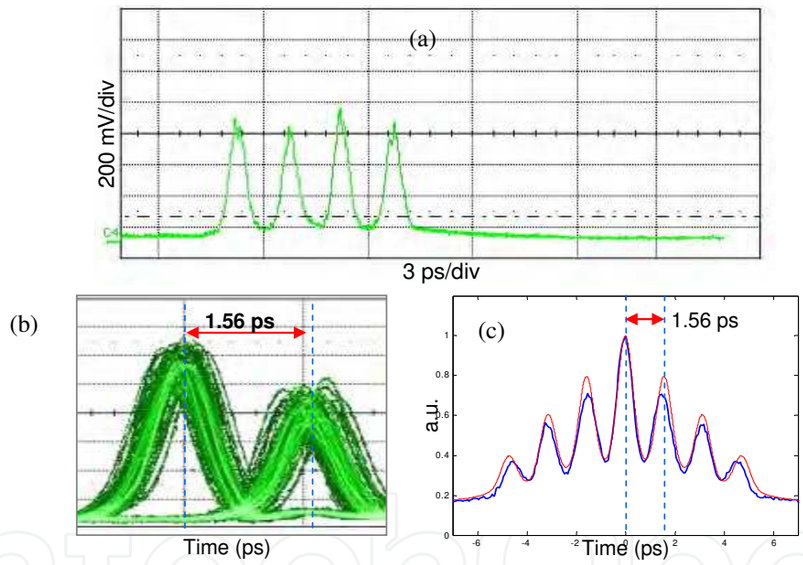


Fig. 21. 640 Gb/s 550 fs RZ pulses sequence evaluated using the optical sampler, visualized on the low-bandwidth oscilloscope after time rescaling (a). Eye-diagram evaluation (b) and comparison between autocorrelation measured through the optical sampler (red thin line) and the one supplied by a commercial autocorrelator (blue thick line) (c).

7. Conclusion

A general view of the optical digital sampling evolution has been reported. Most used optical sampling techniques are described in terms of solutions to obtain timing information and nonlinear interaction to generate sampling gate. In particular the implementation of synchronous, quasi-synchronous and asynchronous schemes exploiting fiber nonlinearities for the sampling gate generation has been described in details.

8. References

Agoston, A.; Pepper, S.; Norton, R.; Ebner, J. & Schoen, K. (2003). 100 GHz through-line sampler system with sampling rates in excess of 10 Gsamples/second, Proceedings of Microwave Symposium Digest, Vol. 3, pp. 1519-1521, ISBN: 0-7803-7695-1, June 2003, IEEE MTT-S International, Philadelphia, PA

Diez, S. Ludwig, R. Schmidt, C. Feiste, U. & Weber, H.G. (1999). 160-Gb/s optical sampling by gain-transparent four-wave mixing in a semiconductor optical amplifier. IEEE Photon. Techonol. Lett., vol. 11, no. 11, Nov. 1999, pp. 1402-1404, ISSN: 1041-1135

Dorrer, C.; Leuthold, J. & Doerr, C.R. (2004). Direct measurement of constellation diagrams of optical sources. Proceedings of OFC 2004, PDP33, ISBN: 1-55752-772-5, Los Angeles, CA, Feb. 2004

Folliot, H.; Lynch, M.; Bradley, A.L.; Krug, T.; Dunbar, L.A.; Hegarty, J.; Donegan, J. F. & Barry, L.P. (2002). Two-photon-induced photoconductivity enhancement in semiconductor microcavities: a theoretical investigation. J. Opt. Soc. Am. B, Vol. 19, No. 10, 2002, pp. 2396-2402.

Fresi, F. Chiuchiarelli, A. Malacarne, A. Potì, L. & Bogoni, A. (2008). 640 Gb/s RZ Eye-Diagram Evaluation by Optical Sampling Oscilloscope w/o Post-Processing and ms Refresh Time. Proceedings of CLEO 2008, CMII5, ISBN: 978-1-55752-859-9, May 2008, San Jose, CA, USA

Jungerman, R.L.; Lee, G.; Buccafusca, O.; Kaneko, Y.; Itagaki, N.; Shioda, R.; Harada, A.; Nihei, Y. & Sucha, G. (2002). 1-THz bandwidth C- and L-band optical sampling with a bit rate agile timebase. IEEE Photon. Technol. Lett., Vol. 14, No. 8, Aug. 2002, pp. 1148-1150, ISSN: 1041-1135.

Kang, I. & Dorrer, C. (2003). Optical sampling source-free simultaneous eye-diagram monitoring and clock recovery up to 160 Gb/s. Proceedings of ECOC 2003, pp. 292–293, Tu4.2.4, Rimini, Italy, Sept. 2003.

Kang, I. & Dreyer, K.F. (2003). Sensitive 320 Gbit/s eye diagram measurements via optical sampling with semiconductor optical amplifier-ultrafast nonlinear interferometer. Electronics Letters, Vol. 39, No. 14, July 2003, pp 1081 – 1083, ISSN: 0013-5194.

Kawanishi, S.; Yamamoto, T.; Nakazawa, M. & Fejer, M.M. 2001. High sensitivity waveform measurement with optical sampling using quasi-phasematched mixing in LiNbO3 waveguide. Electron. Lett., Vol. 37, No. 13, June 2001, pp. 842–844, ISSN: 0013-5194

Krug, T.; Lynch, M.; Bradley, A.L.; Donegan, J.F.; Barry, L.P.; Folliot, H.; Roberts, J.S. & Hill, G. (2004). High-sensitivity two-photon absorption microcavity autocorrelator. IEEE Photonics Technol. Lett., Vol. 16, No. 6, June 2004, pp. 1543–1544, ISSN 1041-1135.

Li, J.; Hansryd, J.; Hedekvist, P.O.; Andrekson, P.A. & Knudsen, S.N. (2001). 300-Gb/s eye-diagram measurement by optical sampling using fiber-based parametric amplification. IEEE Photon. Technol. Lett., Vol. 13, No. 9, Sep 2001, pp. 987-989, ISSN: 1041-1135

Li, J.; Westlund, M.; Sunnerud, H.; Olsson, B.-E.; Karlsson, M. & Andrekson, P.A. (2004).0.5-Tb/s eye-diagram measurement by optical sampling using XPM-induced wavelength shifting in highly nonlinear fiber. IEEE Photon. Technol. Lett., Vol. 16, No. 2, Feb. 2004, pp. 566-568, ISSN: 1041-1135.

Maguire, P.J.; Barry, L.P.; Krug, T.; Lynch, M.; Bradley, A.L.; Donegan, J.F. & Folliot, H. (2005). All-optical sampling utilising two-photon absorption in semiconductor microcavity. Electronics Letters, Vol. 41, No. 8, Apr. 2005, pp.489 – 490, ISSN: 0013-5194.

Malacarne, A. Fresi, F. Meloni, G. Poti, L. & Bogoni, A. (2007). Implementation of a Quasi-Asynchronous sub-ps-resolution all-optical sampler for long bit sequences view without post-processing, Proceedings of LEOS 2007, pp. 920-921, ISBN: 978-1-4244-0925-9, Oct 2007, Lake Buena Vista, Florida

Meloni, G. Bogoni, A. & Potì, L. (2005). Real-time ps-resolution optical sampler based on XPM-induced polarization rotation in 1-meter-long bismuth oxide fibre. Proceedings of ECOC 2005, Vol. 1, pp. 63- 64, ISBN: 0-86341-543-1, Sept 2005, Glasgow

Miyazaki, T. & Kubota, F. (2003). Simultaneous demultiplexing and clock recovery for 160 Gb/s OTDM signal using a symmetric Mach-Zehnder switch in electrooptic feedback loop. IEEE Photon. Technol. Lett., Vol. 15, No. 7, July 2003, pp. 1008–1010, ISSN: 1041-1135

Nogiwa, S.; Kawaguchi, Y.; Ohta, H. & Endo, Y. (2000). Highly sensitive and time-resolving optical sampling system using thin PPLN crystal. Electron. Lett., Vol. 36, No. 20, Sept. 2000, pp. 1727–1728, ISSN: 0013-5194.

Nogiwa, S.; Ohta, H.; Kawaguchi, Y. & Endo, Y. (1999). Improvement of sensitivity in optical sampling system. Electron. Lett., Vol. 35, No. 11, May 1999, pp. 917–918, ISSN: 0013-5194.

Ohta, H. Banjo, N. Yamada, N. Nogiwa, S. & Yanagisawa, Y. (2001). Measuring eye diagram of 320 Gbit/s optical signal by optical sampling using passively modelocked fibre laser. Electron. Lett., Vol. 37, No. 25, Dec. 2001, pp. 1541–1542, ISSN: 0013-5194.

Ohta, H.; Nogiwa, S., Kawaguchi, Y. & Endo, Y. (2000). Measurement of 200 Gbit/s optical eye diagram by optical sampling with gain-switched optical pulse. Electron. Lett., Vol 36, No. 8,Apr. 2000, pp. 737– 739, ISSN: 0013-5194.

Otani, A.; Otsubo, T. & Watanabe, H. (1999). A turn-key-ready optical sampling oscilloscope by using electro-absorption modulators. Proceedings of ECOC 1999, pp. 374–375, Nice, France, September 1999.

Schmidt, C.; Futami, F.; Watanabe, S.; Yamamoto, T.; Schubert, C.; Berger, J.; Kroh, M.; Ehrke, H.-J.; Dietrich, E.; Burner, C.; Ludwig, R. & Weber, H.G. (2002). Complete optical sampling system with broad gap-free spectral range for 160 Gbit/s and 320 Gbit/s and its application in a transmission system. Proceedings of OFC 2002, pp. 528–530, ISBN: 1-55752-701-6, Anaheim, USA, Mar 2002.

Schmidt, C.; Schubert, C.; Watanabe, S.; Futami, F.; Ludwig, R.; & Weber, H.G. (2002). 320 Gb/s All-Optical Eye Diagram Sampling using Gain-Transparent Ultrafast-Nonlinear Interferometer (GT-UNI). Proceedings of ECOC 2002, ISBN: 87-90974-63-8, Copenhagen, Denmark, September 2002.

Schmidt-Langhorst, C & Weber, H. G. (2005). Optical Sampling Techniques, In: J. of Optical and Fiber Communications Research, ed. Springer New York, pp. 86-114, ISSN 1867-3007

Schmidt-Langhorst, C.; Schubert, C.; Boerner, C.; Marembert, V.; Ferber, S.; Ludwig, R. & Weber, H.G. (2005). Optical sampling system including clock recovery for 320 Gbit/s DPSK and OOK data signals. Proceedings of OFC 2005, OWJ6, ISBN 1-55752-783-0, Washington DC, March 2005.

Shake, I Takara, H. & Kawanishi, S. (2003). Simple Q factor monitoring for BER estimation using opened eye diagrams captured by high-speed asynchronous electrooptical sampling. IEEE Photon. Technol. Lett., Vol. 15, No.4, Apr. 2003, pp. 620-622, ISSN: 1041-1135

Shake, I.; Kasahara, R.; Takara, H.; Ishii, M.; Inoue, Y.; Ohara, T.; Hibino, Y. & Kawanishi, S. (2003). WDM signal monitoring utilizing asynchronous sampling and wavelength selection based on thermo-optic switch and AWG. Proceedings of ECOC 2003, pp. 780–781, We4.P112, Rimini, Italy, Sept. 2003.

Shirane, M.; Hashimoto, Y.; Yamada, H. & Yokoyama, H. (2000). A compact optical sampling measurement system using mode-locked laser-diode modules. IEEE Photon. Technol. Lett., Vol. 12, No. 11, Nov. 2000, pp. 1537–1539, ISSN: 1041-1135.

Takara, H.; Kawanishi, S. & Saruwatari, M. (1996). Optical signal eye diagram measurement with subpicosecond resolution using optical sampling," Electron. Lett., Vol. 32, No. 15, Jul 1996, pp. 1399–1400, ISSN: 0013-5194.

Takara, H.; Kawanishi, S.; Yokoo, A.; Tomaru, S.; Kitoh, T. & Saruwatari, M. (1996). 100 Gbit/s optical signal eye-diagram measurement with optical sampling using organic nonlinear optical crystal. Electron. Lett., Vol. 32, No. 24, Nov 1996, pp. 2256–2258, ISSN: 0013-5194.

Tong, D.T.K. Deng, K.-L. Mikkelsen, B. Raybon, G. Dreyer, K.F. & Johnson, J.E. (2000). 160 Gbit/s clock recovery using electroabsorption modulator-basedphase-locked loop. Electron. Lett., vol. 36, no. 23, Nov. 2000, pp. 1951-1952, ISSN: 0013-5194

Uhua, L. Cheolhwan, K. Guifang, L. Kaneko, Y. Jungerman, R.L. & Buccafusca, O. (2003). Wavelength and polarization insensitive all-optical clock recovery from 96-Gb/s data by using a two-section gain-coupled DFB laser. IEEE Photon Technol. Lett., vol. 15, no. 4, Apr. 2003, pp. 590-592, ISSN: 1041-1135

Von der Linde, D. (1986). Characterization of the noise in continuosly operating modelocked lasers, *Journal of Applied Physics B: Lasers and Optics*, Vol. 39, No. 4, April 1986, pp. 201–217, ISSN 0946-2171.

Watanabe, S.; Okabe, R.; Futami, F.; Hainberger, R.; Schmidt-Langhorst, C.; Schubert, C. & Weber, H. G. (2004). Novel fiber kerr-switch with parametric gain: Demonstration of optical demultiplexing and sampling up to 640 Gb/s. Proceedings of ECOC 2004, Th4.1.6, Stockholm, Sweden, Sept. 2004.

Westlund, M. Andrekson, P.A. Sunnerud, H. Hansryd, J. & Jie, L. (2005). High-performance optical-fiber-nonlinearity-based optical waveform monitoring. IEEE J. of Lightwave Technol., Vol. 23, No. 6, June 2005, pp 2012 – 2022, ISSN: 0733-8724

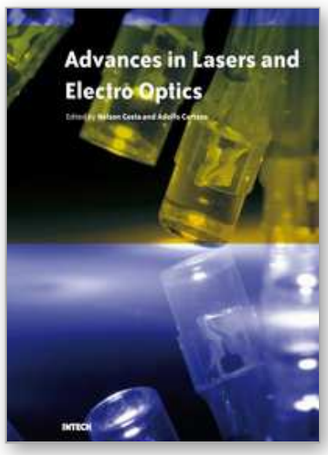
Westlund, M. Sunnerud, H. Karlsson, M. & Andrekson, P.A. (2005). Software-synchronized all-optical sampling for fiber communication systems. IEEE J. of Lightwave Technol., Vol. 23, No. 3, Mar 2003, pp.1088 - 1099, ISBN: 1-55752-746-6

Tektronix Application Notes. (2001). XYZs of Oscilloscope, www.tek.com.

Yamada, N.; Nogiwa, S. & Ohta H. (2004). 640-Gb/s OTDM Signal Measurement With High-Resolution Optical Sampling System Using Wavelength-Tunable Soliton Pulses. IEEE Photon. Technol. Lett., Vol. 16, No. 4, April 2004, pp. 1125-1127, ISSN: 1041-1135.

Yamada, N.; Ohta, H. & Nogiwa, S. (2002). Jitter-free optical sampling system using passively modelocked fibre laser. Electron. Lett., Vol. 38, No. 18, Aug. 2002, pp. 1044–1045, ISSN: 0013-5194.

Yamamoto, T. Oxenlowe, L.K. Schmidt, C. Schubert, C. Hilliger, E. Feiste, U. Berger, J. Ludwig, R. & Weber, H.G. (2001). Clock recovery from 160 Gbit/s data signals using phase-locked loop with interferometric optical switch based on semiconductor optical amplifier", Electron Lett., vol. 37, no. 8, Apr 2001, pp. 509-510, ISSN: 0013-5194



Advances in Lasers and Electro Optics

Edited by Nelson Costa and Adolfo Cartaxo

ISBN 978-953-307-088-9
Hard cover, 838 pages
Publisher InTech
Published online 01, April, 2010
Published in print edition April, 2010

Lasers and electro-optics is a field of research leading to constant breakthroughs. Indeed, tremendous advances have occurred in optical components and systems since the invention of laser in the late 50s, with applications in almost every imaginable field of science including control, astronomy, medicine, communications, measurements, etc. If we focus on lasers, for example, we find applications in quite different areas. We find lasers, for instance, in industry, emitting power level of several tens of kilowatts for welding and cutting; in medical applications, emitting power levels from few milliwatt to tens of Watt for various types of surgeries; and in optical fibre telecommunication systems, emitting power levels of the order of one milliwatt. This book is divided in four sections. The book presents several physical effects and properties of materials used in lasers and electro-optics in the first chapter and, in the three remaining chapters, applications of lasers and electro-optics in three different areas are presented.

How to reference

In order to correctly reference this scholarly work, feel free to copy and paste the following:

Gianluca Berrettini, Antonella Bogoni, Francesco Fresi, Gianluca Meloni and Luca Poti (2010). Evolution of Optical Sampling, Advances in Lasers and Electro Optics, Nelson Costa and Adolfo Cartaxo (Ed.), ISBN: 978-953-307-088-9, InTech, Available from: http://www.intechopen.com/books/advances-in-lasers-and-electro-optics/evolution-of-optical-sampling

INTECH
open science | open minds

InTech Europe
University Campus STeP Ri
Slavka Krautzeka 83/A
51000 Rijeka, Croatia
Phone: +385 (51) 770 447
Fax: +385 (51) 686 166
www.intechopen.com

InTech China
Unit 405, Office Block, Hotel Equatorial Shanghai
No.65, Yan An Road (West), Shanghai, 200040, China
中国上海市延安西路65号上海国际贵都大饭店办公楼405单元
Phone: +86-21-62489820
Fax: +86-21-62489821

© 2010 The Author(s). Licensee IntechOpen. This chapter is distributed under the terms of the Creative Commons Attribution-NonCommercial-ShareAlike-3.0 License, which permits use, distribution and reproduction for non-commercial purposes, provided the original is properly cited and derivative works building on this content are distributed under the same license.

IntechOpen

IntechOpen